ELSEVIER

Journal of Alloys and Compounds 253–254 (1997) 515–519

Journal of ALLOYS AND COMPOUNDS

Hydrogen adsorption of metal nickel and hydrogen storage alloy electrodes

Xueping Gao, Jian Liu, Shihai Ye, Deying Song*, Yunshi Zhang

Institute of New Energy Material Chemistry, Nankai University, Tianjin, 300071, China

Abstract

An improvement in the electrocatalytic activity of the hydrogen storage alloy electrodes is essential to ensure a high rate capability of an Ni–MH battery. Previous experimental results showed that there was a hydrogen adsorption phenomenon on the alloy surface and the activation energy barrier of the electrochemical reaction process should be reduced by hydrogen adsorption. Therefore, the hydrogen adsorption is of benefit in improving the electrocatalytic activity of the alloy electrode. In this work, the hydrogen adsorption performance on the surfaces of $Zr(V_{0.2}Mn_{0.2}Ni_{0.6})_{2.4}$, $MmNi_{3.6}Mn_{0.4}Co_{0.75}Al_{0.25}$ alloy electrodes and carbonyl nickel electrode was measured by means of cyclic voltammetry. In addition, the hydrogen adsorption performance of the metal nickel ribbon was performed by electrochemical impedance spectra. The results showed that the Ni sites on the surface of the metal hydride electrodes play an important role in the hydrogen adsorption.

Keywords: Hydrogen adsorption; Metal hydride electrode; Electrochemical impedance; Cyclic voltammetry

1. Introduction

Nickel-metal hydride batteries have been developed and commercialized because of their high energy density and their environmental advantages. $LaNi_5$-based alloys and Laves phase alloys have been applied to metal hydride electrodes. Recently, new interest in such electrode materials has arisen with respect to the improvement in the electrocatalytic activity and hydrogen adsorption performance on the alloy surface [1–3].

The purpose of the present paper is to examine the hydrogen adsorption phenomenon on the surface of the metal nickel electrode and metal hydride electrode. In addition, the role of Ni sites on the alloy surface in the electrochemical reaction has been discussed.

2. Experimental details

The $Zr(V_{0.2}Mn_{0.2}Ni_{0.6})_{2.4}$ and $MmNi_{3.6}Mn_{0.4}Co_{0.75}Al_{0.25}$ alloys were prepared by arc melting in an argon atmosphere. The alloys were mechanically crushed and ground to 300 mesh particle size without annealing. The $Zr(V_{0.2}Mn_{0.2}Ni_{0.6})_{2.4}$ alloy powder was treated by HF acid solution [4]. The surface chemical state and composition of the untreated and treated alloy powders were measured by means of XPS.

The metal nickel ribbon was mechanically polished with No. 600 silicon carbide waterproofed paper. The nickel ribbon back and spot-welded nickel wire were sealed with epoxy resin to give an electrode apparent surface area of 4.0 cm^2. The electrode was treated with hot concentrated H_2SO_4 and hot 1 M NaOH solution in order to remove the oxide film and greasy dirt on the surface. The cathodic polarization of the electrode was carried out under current density of 25 $mA\,cm^{-2}$ for 1 h in a three compartment glass electrolysis cell with a Hg/HgO(5 M KOH) electrode as reference electrode. After that, the electrochemical impedance spectra of the metal nickel electrode were measured using a Solartron 1250 frequency response analyzer in combination with a TD3690 potentiostat at a different polarization condition. The impedance spectra of the metal nickel electrode were recorded from 10 kHz to 10 mHz and at 5 mV of the amplitude of perturbation. The impedance spectra were fitted to an equivalent circuit using a non-linear, least-squares (NLLS) fitting program EQUIVCRT [5].

The cyclic voltammetry experiments of the metal hydride electrodes were taken using a TD3690 potentiostat, controlled by an external computer. A three-electrode system with a Hg/HgO(5 M KOH) reference electrode and a platinum wire counterelectrode was used. The working electrodes were constructed from an approximate apparent

---

*Corresponding author.

0925-8388/97/$17.00
PII S0925-8388(96)03034-4

surface of 1.0 cm^2 plates of alloy powders without carbonyl nickel powder. After activation with constant current charge–discharges, the cyclic voltammograms of these electrodes were performed.

3. Results and discussion

3.1. Hydrogen adsorption of the metal nickel electrode

Previous work has demonstrated that there was a hydrogen adsorption phenomenon on the surface of both metal electrode and metal hydride electrodes in the electrochemical reaction [6]. In order to further investigate the hydrogen adsorption on the metal surface, the electrochemical impedance spectra of the metal nickel ribbon electrode were examined at different potentials, as shown in Fig. 1.

The impedance spectrum in Nyquist plot representation for the metal nickel at the potential of −950 mV mainly consisted of obvious semicircles and a slope related to the Warburg impedance. The high-frequency region semicircle was attributed to the surface charge transfer process. The low-frequency region slope meant that there was a hydrogen diffusion process. This result showed analogies to the impedance spectrum of the treated $Zr(V_{0.2}Mn_{0.2}Ni_{0.6})_{2.4}$ alloy electrode at the lower hydrogen content [4]. At the potential of −1050 mV, the impedance spectrum almost consisted of a semicircle. This result indicated that the charge-transfer process was the rate-determining step. With increases in the potential, the hydrogen adsorption phenomenon was observed at low frequencies for all impedance spectra. Firstly, the hydrogen adsorption in the low frequency mainly existed as an inductive reactance type at the potentials of both −1100 mV and −1200 mV. In addition, the semicircle of inductive reactance type was

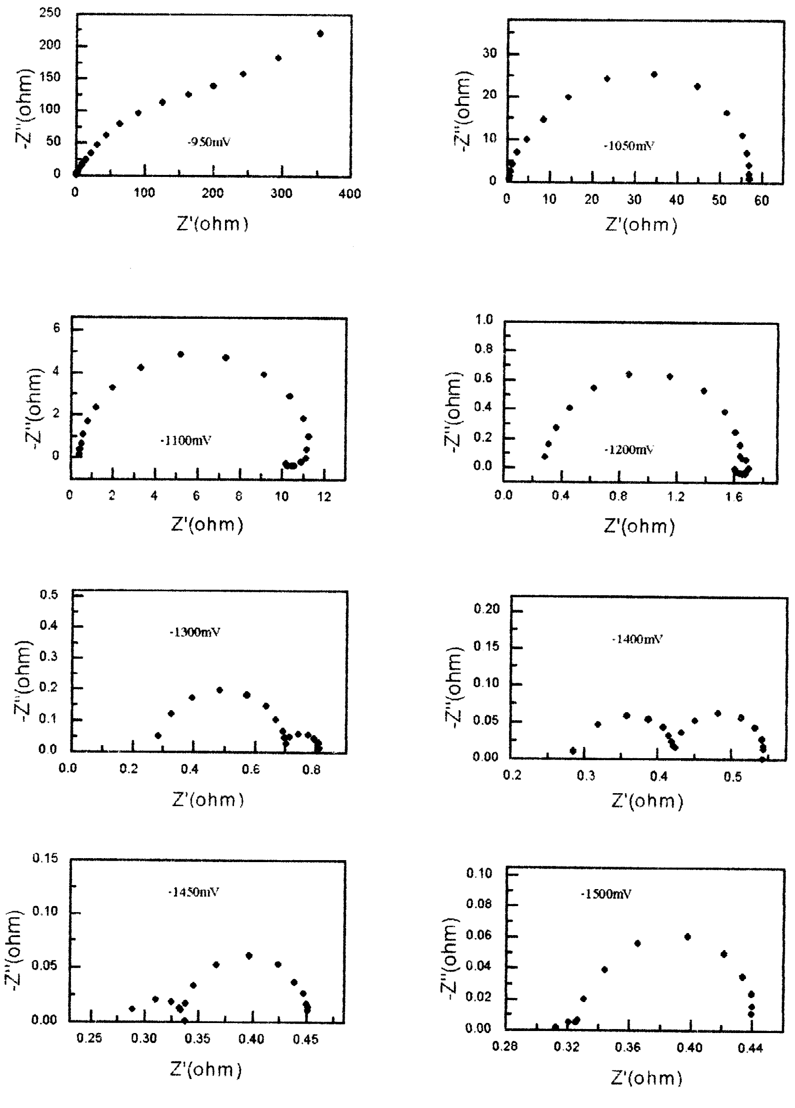

Fig. 1. Electrochemical impedance spectra of a metallic nickel ribbon electrode at different potentials.

progressively rotated. Secondly, the semicircle at low frequency was changed from an inductive reactance type to a capacitive reactance type with increasing potentials. Furthermore, the semicircle at the high frequency became smaller and the semicircle for the capacitive reactance type at the low frequency became larger by comparison. In particular, the electrochemical process was under the control of the hydrogen adsorption in the potential of −1500 mV. This phenomenon showed that the hydrogen adsorption plays an important role in cathodic polarization of the metal nickel electrode. The measured and simulated impedance spectra and their equivalent circuits for the hydrogen adsorption systems of both the inductive reactance type (−1100 mV) and the capacitive reactance type (−1300 mV) are shown in Fig. 2.

3.2. Hydrogen adsorption on metal hydride electrodes

Cyclic voltammetry has been a powerful tool for investigating the adsorption phenomenon of various electrochemical systems [7]. It is well known that the reaction process of the hydride electrode involved two main steps, i.e. a surface charge transfer process and a solid phase hydrogen diffusion process. The product (hydrogen) of the charge-transfer process was adsorbed on the surface of the hydride electrode. Our previous work showed that the Ni sites on the surface of the F-treated $Zr(V_{0.4}Ni_{0.6})_{2.4}$ alloy electrode were hydrogen adsorption centres [3]. In order to demonstrate this reaction mechanism of the hydride electrode, the CVs of both $Zr(V_{0.2}Mn_{0.2}Ni_{0.6})_{2.4}$ and $MmNi_{3.6}Mn_{0.4}Co_{0.75}Al_{0.25}$ alloy electrodes were measured after activation with constant current charge–discharge and are presented in Fig. 3. For the $Zr(V_{0.2}Mn_{0.2}Ni_{0.6})_{2.4}$ alloy treated with a HF solution, there was a strong hydrogen adsorption peak, as found in $Zr(V_{0.4}Ni_{0.6})_{2.4}$ electrodes treated in HF solution [3]. This phenomenon was also attributed to the metallic nickel-rich surface of the treated alloy electrode, as mentioned in our previous work (Ni atomic concentration was increased from 15% to 78%) [4]. The nickel content on the top surface of the $MmNi_{3.6}Mn_{0.4}Co_{0.75}Al_{0.25}$ alloy electrode was poor compared with other constituents such as Mm, Co and Al examined using XPS (atomic concentration Ni 16%; Mm 18%; Co 38%; Al 23%). However, the hydrogen adsorption peak on the surface of the $MmNi_{3.6}Mn_{0.4}Co_{0.75}Al_{0.25}$ alloy electrode was still found at the cathodic direction near the same potential position. This was attributed to the difference in the surface structure between the Laves phase alloy and the $MmNi_5$-based alloy. It was known that a compact thin passive ZrO_2 layer on the Laves phase alloy surface prevents water dissociation and hydrogen adsorption and penetration. After the treatment using the HF solution, the metallic nickel-rich surface of the Laves phase alloy electrode was obtained and the electrocatalytic activity and hydrogen adsorption performance were improved by comparison.

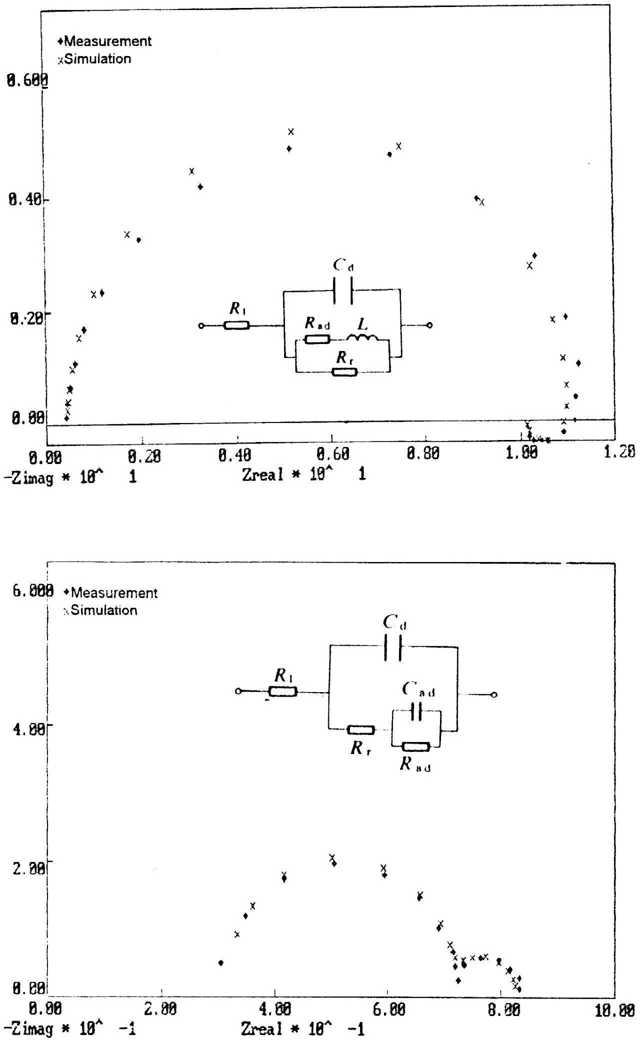

Fig. 2. Measured and simulated impedance spectra and their equivalent circuits for the hydrogen adsorption systems of inductive reactance type (−1100 mV) and capacitive reactance type (−1300 mV).

For $LaNi_5$ alloys, Schlapbach [8] found that the dissociate chemisorption of H_2 can occur at the metallic nickel particles or at the metallic subsurface of $LaNi_5$. The presence of a metallic nickel-rich layer (face-centred cubic structure) at the subsurface of $LaNi_5$ was clearly seen using TEM by De Veirman et al. [9]. The surface orbitals of fcc nickel were considered to define the stereochemistry of adsorption and possible adsorption sites [7]. By analogy, one can also consider that hydrogen easily penetrates and is adsorbed at the Ni sites on the surface or subsurface via the loosely bound oxide layers on the $MmNi_5$-based alloy electrode. In brief, the metallic nickel-rich layer on the surface of both Laves phase and $MmNi_5$-based alloy electrodes is the important factor for hydrogen adsorption. The hydrogen adsorption is of benefit for improving the electrocatalytic activity of the metal hydride electrode since it reduces the activation energy barrier of the electrochemical reaction, as shown in Fig. 4.

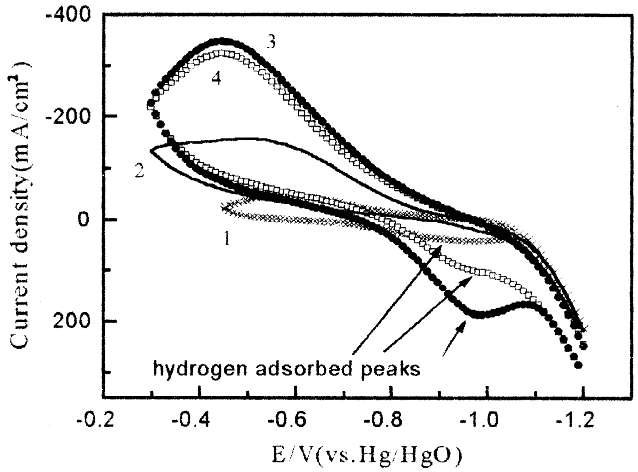

Fig. 3. The CVs of MH electrodes and carbonyl nickel electrode. (1) Carbonyl nickel electrode (scan rate 100 mV s^{-1}). (2) $Zr(V_{0.2}Mn_{0.2}Ni_{0.6})_{2.4}$ alloy electrode (scan rate 30 mV s^{-1}). (3) $Zr(V_{0.2}Mn_{0.2}Ni_{0.6})_{2.4}$ alloy electrode by HF treatment (scan rate 30 mV s^{-1}). (4) $MmNi_{3.6}Mn_{0.4}Co_{0.75}Al_{0.25}$ alloy electrode (scan rate 30 mV s^{-1}).

Fig. 5a shows that the peak potential and peak current of the hydrogen adsorption on the metallic nickel-rich surface of the $Zr(V_{0.2}Mn_{0.2}Ni_{0.6})_{2.4}$ alloy electrode hardly changes with increasing steady-state potential at a constant scan rate. A similar tendency can be observed for the $MmNi_5$-based alloy electrode in Fig. 5b, although the peak current of the hydrogen adsorption increases slightly with increasing steady-state potential. It is probably due to a fast hydrogen diffusion rate across the surface of the metal hydride electrode.

4. Conclusions

For the metal nickel electrode, the hydrogen adsorption on the surface is of inductive reactance type and a capacitive reactance type as shown by electrochemical impedance spectra. For metal hydride electrodes, hydrogen adsorption was obtained on both the metallic nickel-rich surface of the Laves phase alloy and the subsurface of the $MmNi_5$-based alloy by CVs. It is suggested that a metallic nickel-rich layer on the surface of the metal hydride electrodes was the important factor for the hydrogen adsorption. The hydrogen adsorption is of benefit for improving the electrocatalytic activity of the metal hydride electrode by reducing the activation energy barrier of the electrochemical reaction. It is important for alloy design and modification of the metal hydride electrode. A novel point worth noting is that the peak potential and peak current of the hydrogen adsorption at the cathodic direction hardly changes with increasing initial steady-state potential or hydrogen concentration.

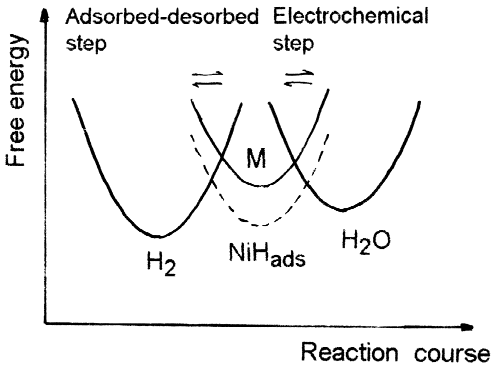

Fig. 4. Influence of the hydrogen adsorption of the Ni-rich surface on the activation energy barrier of the metal hydride electrode reaction.

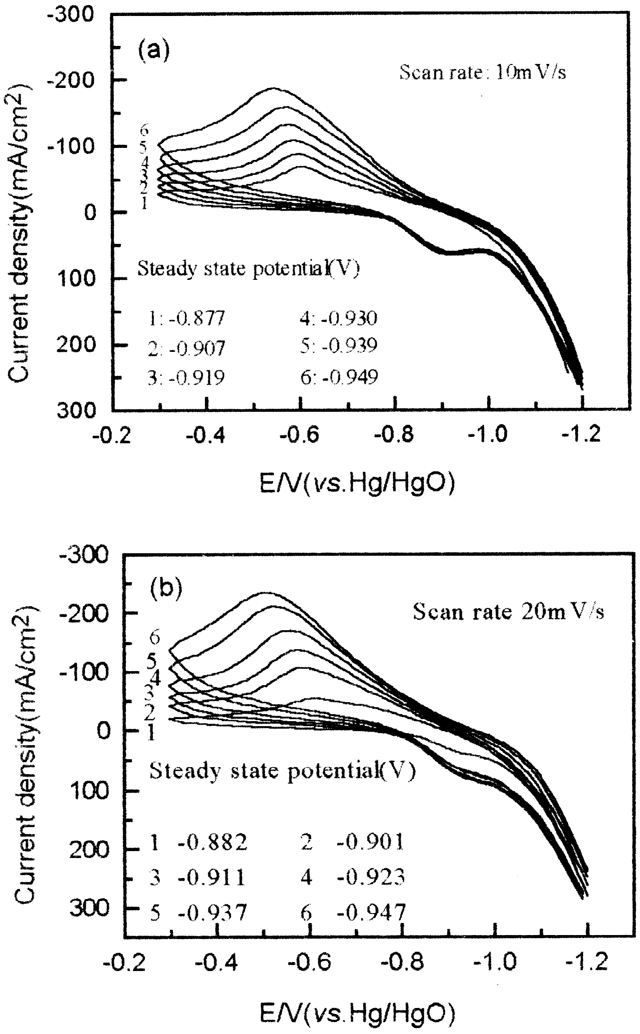

Fig. 5. Cyclic voltammograms at different initial steady-state potentials: (a) $Zr(V_{0.2}Mn_{0.2}Ni_{0.6})_{2.4}$ alloy electrode after HF treatment; (b) $MmNi_{3.6}Mn_{0.4}Co_{0.75}Al_{0.25}$ alloy electrode.

Acknowledgments

This work was supported by the National Advanced Material Committee of China (NAMCC).

References

[1] P.H.L. Notten and R.E.F. Einerhand, *Adv. Mater., 3(7-8)* (1991) 343.
[2] B.E. Conway and G. Jerkiewicz, *Z. Phys. Chem., 183* (1994) 281.
[3] X.P. Gao, W. Zhang, H.B. Yang, D.Y. Song, Y.S. Zhang, Z.X. Zhou and P.W. Shen, *J. Alloys Comp., 235* (1996) 225.
[4] X.P. Gao, D.Y. Song, Y.S. Zhang, Z.X. Zhou, W. Zhang and P.W. Shen, *J. Alloys Comp., 229* (1995) 268.
[5] B.A. Boukamp, *Solid State Ionics, 20* (1986) 31.
[6] K.L. Hardee and A.J. Bard, *J. Electrochem. Soc., 123* (1976) 1024.
[7] A.J. Bard and L.R. Faulkner, *Electrochemical Methods*, John Wiley, 1980, p. 523.
[8] F. Meli and L. Schlapbach, *J. Less-Common Met., 172–174* (1991) 1252.
[9] A.E.M. De Veirman, A.A. Staals and P.H.L. Notten, *Phil. Mag. A, 70* (1994) 837.